ELSEVIER

International Journal of Heat and Fluid Flow 22 (2001) 519–524

International Journal of HEAT AND FLUID FLOW

www.elsevier.com/locate/ijhff

Flow dynamics between the inclined fins of a finned tube

I. Carvajal-Mariscal [a,b,*], F. Sanchez-Silva [a,b], P. Quinto-Diez [a,b]

[a] *Thermal Hydraulics Applied Engineering Laboratory, National Polytechnical Institute, Mexico*
[b] *SEPI-ESIME-IPN, Edif. 5 – 3rd floor, UPALM, 07738 Mexico D.F., Mexico*

Received 12 August 2000; accepted 31 January 2001

Abstract

An experimental program was undertaken to measure the local static pressure along an inclined fin's internal and external faces on a finned tube provided with these devices; the airflow was transversal to the tube. The fins inclination angle respect to the tube axis was 45°. The local static pressure on the tube surface between a pair of fins was also measured; the experimental results are presented and analysed in this paper. The analysis indicates the presence of volumetric streams (secondary flows) in the internal side channel formed by two inclined fins. On the external fin's face, the flow has a similar tendency as in the cylinder case but with a late detachment of the boundary layer in the fin's tip. With the local static pressure distribution measured, it was possible to evaluate the drag coefficient C_D for the internal and external faces of the inclined fins and on the tube surface as well, for a range of velocities ($Re_d = 6–56 \times 10^3$). The results of the drag coefficient computed for the inclined fins were compared against other authors' results, for a smooth cylinder and a sphere, and we can conclude that for the finned tube with inclined fins the aerodynamic resistance is nearly 1.5 times higher than the one encountered for a smooth cylinder case.

Keywords: Inclined fins; Secondary flow; Flow-field measurement

1. Introduction

Increasing the thermal efficiency of heat exchangers is a problem existing since the invention of the thermal equipment and systems. At present, solving this problem is very important especially for the heat exchangers using gases as agents for heat transfer, due to their low-density thermal flow. This kind of exchangers generally have a large surface for heat exchange, some examples are: eolic condensers, heat recovery steam generators, heating and cooling air systems, economisers in the steam generators and others.

The heat transfer improvement of a heating surface is a problem including several factors. Among the main factors there are the fin type and its shape selection, but it is also important the optimal relationship between the heat transfer, the pressure drop due to the aerodynamic resistance and the compactness of the surface.

Several studies on the fins thermal efficiency have been carried out, among them there are those experimental and theoretical investigations of Pismennyi (1991, 1994) on the flow behaviour and the heat transfer coefficient distribution over straight fin surfaces on bank of tubes, and the investigation about the spacing effect on the convection on plate and tube finned heat exchangers (Romero-Méndez et al., 2000). Besides some methods to intensify the convective heat transfer coefficient in extended surfaces using non-conventional fin geometries were analysed by Pismennyi (1996).

In this paper, we propose to extend the heating surface in order to intensify the heat transfer by inclining the radial fin an angle γ, respect to the axis of the tube (Fig. 1). For a bank of tubes, there is some recovered space between the tubes as a result of the fins inclination. This recovered space could be used in two ways: first to diminish the distance between tubes and second to increase the fin's height. The second action is possible because the fin inclination reduces the mechanical tension in their sharp tip, avoiding its crash when it is placed around the tube.

Pronin and Carvajal-Mariscal (1996) have shown experimentally that by inclining, an angle γ respect to the tube axis, the squared cross-section radial fins, it is possible to increase the compactness β (relationship between the surface A and its volume V) of a bank of finned tubes when they have a dense distribution (Fig. 2). At the same time, lengthen the inclined fin height H augments even more the compactness of the bank of tubes as shown by line 2 in Fig. 2, in comparison with the case when the transversal and longitudinal tube pitch ($S_p \times S_n$) are reduced in a squared shifted matrix very dense, see line 1 in Fig. 2.

The above results encouraged the heat transfer research in this kind of surfaces. First of all, it was decided to study the aerodynamic characteristics of the tubes with inclined fins in order to have basic information for the future application in heat transfer equipment.

* Corresponding author.

0142-727X/01/$ - see front matter
PII: S0142-727X(01)00106-0

Notation

v	kinematic viscosity (m^2/s)
β	compactness (m^2/m^3)
δ	fin thickness (m)
γ	inclination angle of fin (°)
φ	revolution angle of the finned tube (°)
A	surface (m^2)
C_D	drag coefficient
C_p	pressure coefficient
d	finned tube diameter (m)
F_A	drag force on the fin surfaces (N)
f_A	projection of the inclined fin surface (m^2)
F_C	drag force on the cylindrical surface (N)
H	height of fin (m)
l	length of the tube (m)
P_φ	local pressure on the surfaces (Pa)
P_0	pressure in front of the finned tube (Pa)
Re_d	$(u \times d)/v$
$S_p \times S_n$	transverse and longitudinal tube pitch (m)
u	flow velocity based on the frontal area (m/s)
V	volume (m^3)

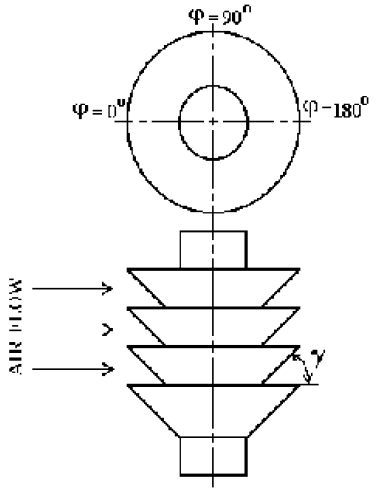

Fig. 1. Tube with inclined fins. γ°: angle of inclination; φ°: revolution angle of the finned tube.

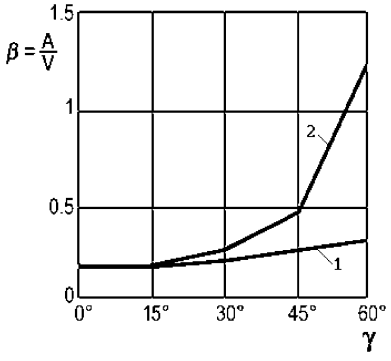

Fig. 2. Effect of inclination angle γ° in the compactness β of a bank of finned tubes with dense disposal. 1: $H = \text{cons.}$, $(S_p \times S_n) = \text{var.}$ 2: $H = \text{var.}$, $(S_p \times S_n) = \text{cons.}$

2. Aerodynamic characteristics of the tubes with inclined fins determination

By inclining the fins and increasing its height, a raise in the aerodynamic resistance of the tubes is previewed. So it is important to determine their drag coefficient so that, they can be used in the design of heat exchangers equipment.

To study the aerodynamic characteristics, a scale model was built. It consisted of a 42 mm diameter tube with inclined fins (Fig. 3). The base of the model was a steel tube (38 mm of

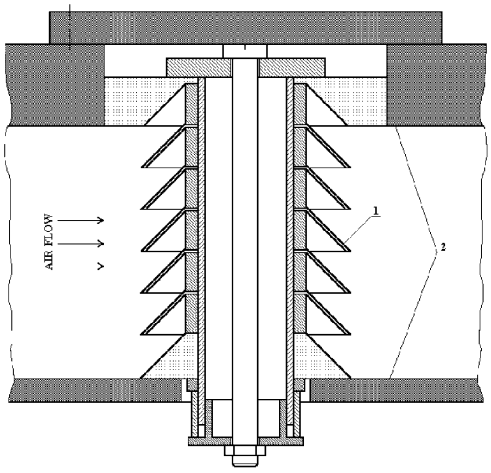

Fig. 3. Model of tube with inclined fins in the experimental channel. 1: Inclined fin with pressure taps. 2: Experimental channel walls.

diameter) in which five plastic fins inclined $\gamma = 45°$ and six metal rings 42×38 mm, 16 mm of height (distance between two fins) were installed. So that, there were six channels between the fins and the experimental channel wall (Fig. 3). The fin's characteristics are: height $H = 20$ mm, thickness $\delta = 2$ mm.

In the central fin of the tube, 16 pressure taps of 0.3 mm diameter were drilled and distributed all along the two faces of the inclined fin (Fig. 4). On both fin faces were distributed 8 pressure taps with a separation of 2 mm between them, starting in the fin's tip. The pressure transmission lines go through a channel, axially inside the tube to a potentiometer. To measure the local static pressure distribution all along the fin surface, the finned tube was twisted around its own axis and for the local static pressure distribution on the cylindrical surface between two fins, three more pressure taps of the same diameter were drilled on this tube surface (Fig. 4). These pressure taps were distributed starting at 4.5 mm from the base of the fin and separated 3.5 mm.

The model was exposed to a transversal airflow in a wind tunnel, which was formed by a 120×106 mm cross-section channel and 950 mm length. The inlet of the channel is formed by rounded tips and it has a chamber for the velocity profile homogenisation before the finned tube. A centrifugal compressor provided air at a rate of 0.5 kg/s and 700 mm water column of gage pressure.

The airflow rate was measured with the help of a subsonic nozzle connected to a U manometer. A manometer with 19 inclined 2 mm diameter tubes was used to measure the static

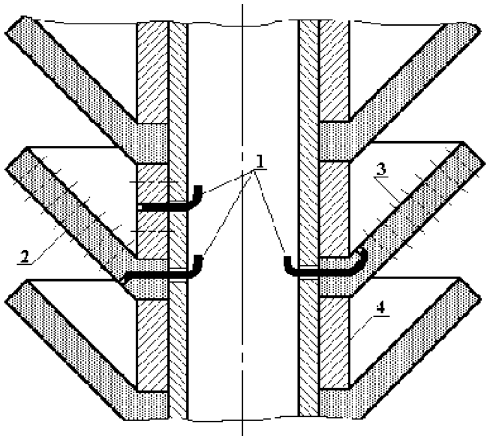

Fig. 4. Distribution of pressure taps on the fins's faces and on the cylindrical surace. 1: Pressure transmission lines. 2: External fin's face. 3: Internal fin's face. 4: Ring for the fin separation.

pressure; this device was built and calibrated in our laboratory. The measurement error using the manometer above described was estimated to be about 3%.

The velocity range of the experiments was $Re_d = (6\text{–}56) \times 10^3$, because is the range more representative for heat exchangers with extended surfaces (Zukauskas, 1982).

3. Experimental results

It is well known that the local static pressure distribution characterises the external flow respect the boundary layer. So, if we know the local static pressure distribution in both faces of the fin and in the cylindrical region between two fins, it is possible to understand the flow characteristics. Then it is also possible to identify the regions of contact and flow detachment, the region where the vortices are formed and also the flow direction in different points of the fin-tube system.

The pressure coefficient C_p was computed using the equation suggested by White (1988):

$$C_p = 1 - \frac{P_0 - P_\varphi}{(1/2)\,\rho\, u^2}. \tag{1}$$

In the plots, φ represents the revolution angle of the finned tube. Due to the geometrical symmetry only half of the circumference is presented.

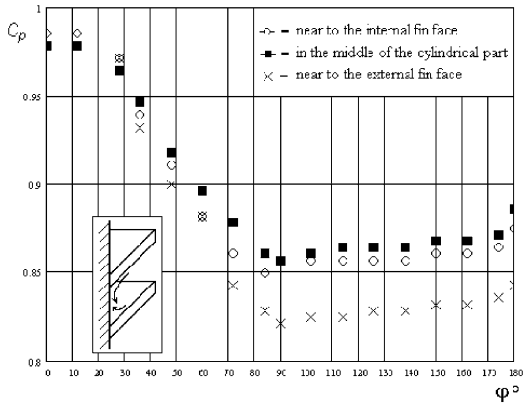

Fig. 6. Distribution of the pressure coefficient C_p on the cylindrical surface for $Re_d = 9000$.

Figs. 5 and 6 show the distribution of the pressure coefficient in the middle and the extremes of the cylindrical zone for two air flow velocities. In the frontal region, the pressure decreases and after $\varphi > 90°$ it increases again. Fig. 5 shows the typical C_p behaviour, in the frontal part ($0° \leqslant \varphi \leqslant 90°$) the flow accelerates and in the rear, there are counter current flows due to the boundary layer separation.

The flow direction at the cylinder in the frontal region of the tube ($0° \leqslant \varphi \leqslant 90°$) is inverted in the rear region ($90° \leqslant \varphi \leqslant 180°$). This fact is shown in Fig. 5, the flow direction is indicated with arrows. We can conclude that this phenomenon is related to the vortex formation in this area.

For Reynolds about $Re_d < 20,000$, this phenomenon disappears. On the other hand, it is possible to observe an abrupt pressure reduction on the rear region ($90° \leqslant \varphi \leqslant 180°$). This means that the current extends toward the neighborhood of the external surface of the fin as shown in Fig. 6.

Fig. 7 shows the pressure coefficient distribution in the tip and in the root of the external fin face for $Re_d = 56{,}000$. There is a similar behaviour of the stream in this face and the one for the cylinder.

It is also possible to remark that the flow detachment in the tip of the fin occurs with delay ($\varphi \approx 100°$) respect to the one observed in the fin root and occurs practically in the same point as in the cylindrical surface ($\varphi \approx 85°$).

The pressure coefficients distributions in the tip and the root of the internal face of the fin are in Figs. 8 and 9 for two

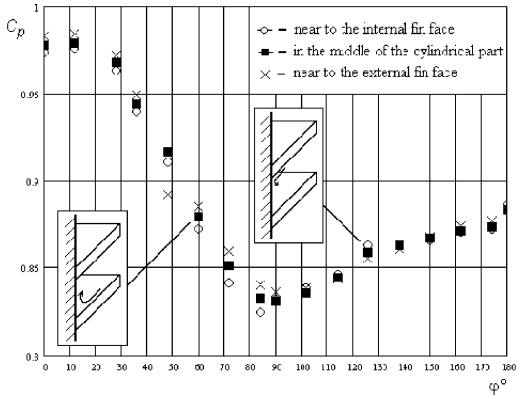

Fig. 5. Distribution of the pressure coeffcient C_p on the cylindrical surface for $Re_d = 56{,}000$.

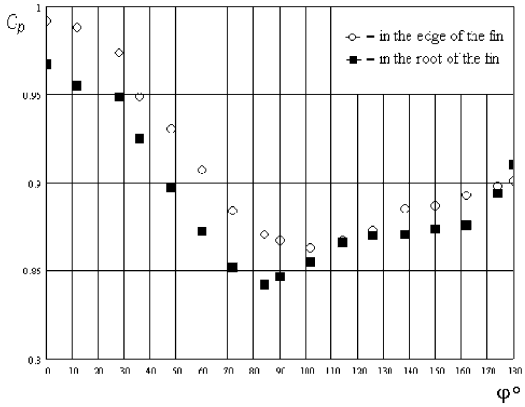

Fig. 7. Distribution of the pressure coefficient C_p on the external fin's face for $Re_d = 56{,}000$.

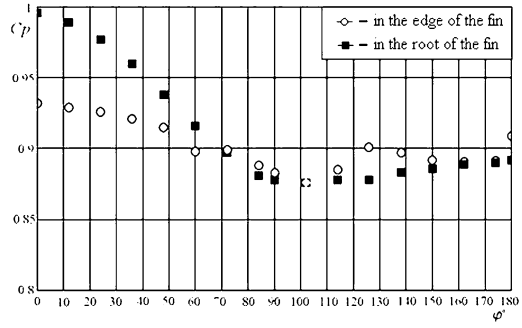

Fig. 8. Distribution of the pressure coefficient C_p on the internal fin's face for $Re_d = 56,000$.

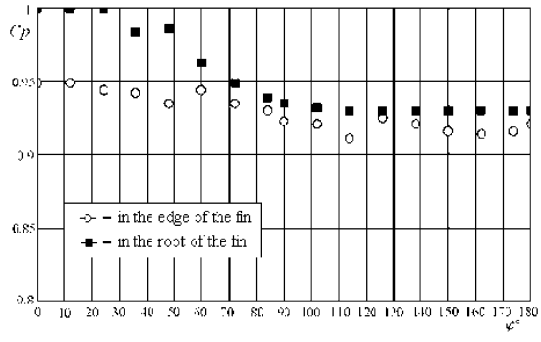

Fig. 9. Distribution of the pressure coefficient C_p on the external fin's face for $Re_d = 8000$.

air velocities, there are vortices in this area that make difficult the flow dynamics.

In Fig. 8 there are some results for $Re_d = 56{,}000$, we can distinguish that in the frontal part ($0° \leqslant \varphi \leqslant 90°$) of the fin, the pressure coefficient values in the root of the fin are lower than in the tip, indicating that the flow accelerates, getting the static pressure its minimum value in the position $\varphi \approx 90°$, when the flow detaches from the surface. Behind this point, the local static pressure has a small increment indicating that there are counter current flows.

In the tip of the fin, the pressure coefficient distribution is very different, presenting a maximum ($\varphi \approx 125°$) and a minimum ($\varphi \approx 100°$) points (Fig. 8). This behaviour indicates the presence of some vortices in this area, which detaches and attaches to the internal face of the fin.

For $Re_d < 9000$ the pressure coefficient distribution, in the root of the internal fin surface, is different than for higher Reynolds, as shown in Fig. 9. In this place the static pressure decreases from the frontal critical point until the point where $\varphi \approx 110°$, after this point it is stable, showing that in this region there is probably a stagnant point provoked by the low velocity of the flow. On the contrary, on the fin tip, there is a similar tendency to the one presented for $Re_d = 56{,}000$ shown in Fig. 8, where there are several detachments and ratachments of the flow with the fin surface.

In order to better understand the flow dynamics on the channel formed by two inclined fins, Fig. 10 shows the point where the distribution of pressure coefficient for the height of the inclined fin is expected to give more information about vortex formation.

In the frontal region of the fin, there is a maximum and a minimum, due to the flow attachment and flow detachment from the fin surface (Fig. 10). In this way, we can consider that

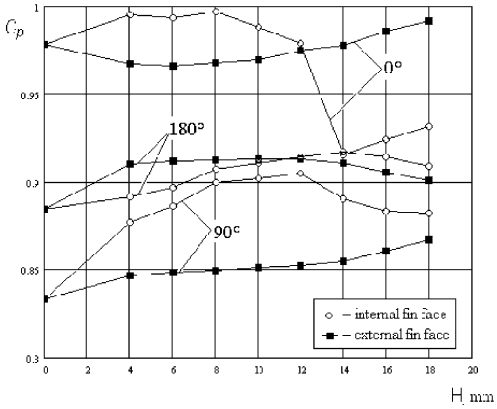

Fig. 10. Distribution of the pressure coefficient C_p for the height of the internal fin's face for $Re_d = 56,000$ at revolution angle of the finned tube $\varphi° = 0°$, 90°, 180°.

vortices are formed not exactly at the tip of the fin but at a certain defined distance (in our case at 6 mm from the tip). The vortex touches the surface at approximately 6 mm from the root. We can conclude that at the middle of the fin there is a recirculation zone.

In the point $\varphi = 90°$ of the fin lateral part, we can observe that the vortices formed in the frontal region of the channel, from external face to internal face, makes contact with the centre of the fin (Fig. 10). At low velocities the contact occurs near the tip of the fin.

In the point $\varphi = 180°$, in the rear region of the tube, the flow coming from the channel formed by two fins creates a recirculation zone as big as 3/4 of the fin length (Fig. 10).

Analysing all the flow dynamics in the channel formed by all the inclined fins, it is shown that the frontal part of the flow, in the internal fin face, is an independent area where the vortices are formed; on the contrary, in the rear part of the channel the flow has a structure which is formed as a result of the created eddies in the internal face of the frontal part and the detachment of the boundary layer in the cylindrical part, and in the external face of the inclined fin as well.

Taking into consideration the local static pressure distribution obtained experimentally at the height of the fin at different rotation angles of the tube, and according to the analysis below exposed, it is possible to propose a physical model for the flow dynamics in the channel formed by the set of inclined fins (Fig. 11).

This model differs from the one obtained for the convectional straight fins presented by Pismennyi (1984, 1991, 1994), where the vortex originated in the frontal side of the tube has a different behaviour in its rear region. In the case of the straight fins, there is not a recirculation zone that covers 3/4 of the fin height when $\varphi = 180°$.

This physical model of the flow dynamics allows us to determine the characteristics and structure of the flow in different regions of the channel, and we can also analyse the reasons of the increment of the aerodynamic resistance, besides, we can distinguish the areas where the eddies are formed and determine their magnitude as well.

4. Drag coefficient of the tube with inclined fins

The drag coefficient in a tube is computed integrating the local static pressure distribution on both fin faces and in the cylindrical surface. The following expressions were used to

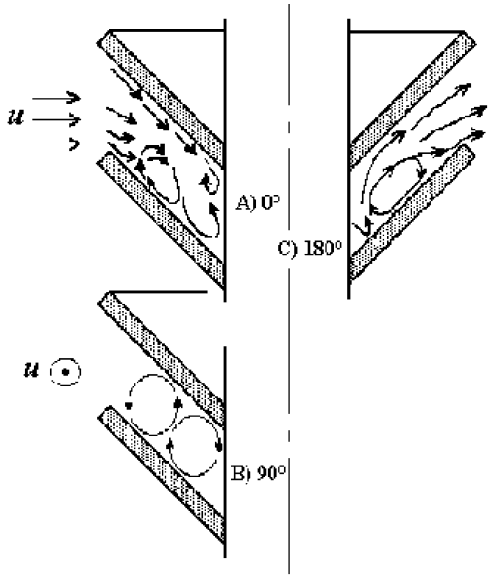

Fig. 11. Physical model of the flow dynamics in the channel formed by the set of inclined fins for different revolution angles $\varphi°$ of the finned tube.

compute the drag coefficient (Holman, 1993), for the cylindrical surface:

$$C_D = \frac{\sum F_C}{dl\rho(u^2/2)} \tag{2}$$

for the inclined fin

$$C_D = \frac{\sum F_A}{f_A \rho\,(u^2/2)}, \tag{3}$$

where F_C and F_A forces were calculated using the experimental static pressure data, obtained on the cylinder surface and on both inclined fin surfaces. For this purpose conventional expressions were used as follows.

In the case of the cylinder the value of F_C corresponds to the static pressure value measured in each point of the surface.

$$F_C = (P_0 - P_\varphi) A_\varphi,$$

where F_A was calculated considering the fin inclination angle; so only the component x of the static pressure on both faces of the fin is considered.

$$F_C = (P_0 - P_\varphi) \cos\gamma A_\varphi,$$

where A_φ is the area around the pressure tap for each angle φ.

The drag coefficient C_D values of the fin in both internal and external faces, and in the cylindrical surface, for different flow velocities are shown in Fig. 12. In this figure the typical drag coefficient values for a smooth tube and a sphere (Schlichting and Gersten, 2000) are compared with the drag coefficient obtained for the tube with inclined fins.

Fig. 12 shows the three main components of the total aerodynamic resistance. The main resistance come from the tube surface. The second important resistance is the external face and finally the one of the internal face. The cylindrical surface and the fin's external face are crossed by high velocity flows, contrary to the internal face of the fin. This explains the drag coefficient values obtained.

The values obtained for a finned cylinder using inclined fins are approximately 1.5 bigger than the ones for a smooth cylinder (Fig. 12), but it is interesting to observe that by

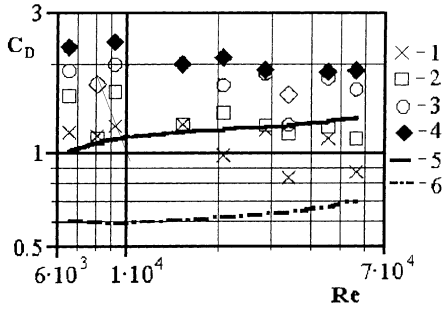

Fig. 12. Drag coefficient C_D of tube's surfaces.1: Internal fin's face. 2: External fin's face. 3: Cylindrical surface. 4: Tube with inclined fins. 5: Smooth tube (Schlichting and Gersten, 2000). 6: Sphere (Schlichting and Gersten, 2000).

increasing the flow velocity over the fined tube, the drag coefficient tends to decrease slowly.

In the case of heat exchanger applications, the inclined fins would be helical, therefore we suppose there will be some variations in the flow dynamics behaviour, for instance in the drag coefficient. We also consider that in the frontal part of the tube, the physical model could be conserved as shown in this paper, but in the rear region an asymmetry will present, part of the flow will touch the internal face of the helical fin and will try to climb to the upper fin. Meanwhile on the other face there will be counter current flows mixing with the flow coming from the lower fin. This situation of high turbulence probably will produce a stagnant zone.

5. Conclusions

From the results obtained for the local static pressure distribution on the tube surfaces with inclined fins and the drag coefficient computation, we can conclude that the heating surfaces formed by these finned tubes will have an aerodynamic resistance barely superior to the one for the tubes with conventional straight fins.

On the other hand, the tubes with inclined fins provide a heating surface with a superior compactness as far as 50% in the case of the inclination angle of $\gamma = 45°$ as shown in Fig. 2. This could compensate the increase of the aerodynamic resistance offered by the surface formed by the tube with inclined fins.

In the near future this research will be oriented to obtain the heat transfer characteristics of the surfaces formed by the tubes with inclined fins.

References

Holman, J.P., 1993. Heat Transfer. McGraw-Hill, NewYork.

Pismennyi, E.N., 1984. Investigation of flow dynamics in surface of fin of cross-finned tube. J. Eng. Phys. 47 (1), 28–31 (in Russian).

Pismennyi, E.N., 1991. Particularities of flow dynamics and heat transfer of convectional cross-finned heat transfer surfaces. J. Eng. Phys. 60 (6), 895–902 (in Russian).

Pismennyi, E.N., 1994. Physical model of flow dynamic and heat transfer of convectional cross-finnned heat transfer surfaces. In: Proceedings of the I Russian National Conference of Heat Transfer, vol. 8, pp. 132–136, vol. 43, pp. 39–51 (in Russian).

Pismennyi, E.N., 1996. Methods for increases effectiveness of cross-finned heat transfer surfaces. In: Proceedings of the III Minsk International Forum for Heat Transfer, vol. 10, pp. 221–225 (in Russian).

Pronin, V.A., Carvajal-Mariscal, I., 1996. Increase of compactness and energy effectiveness of convectional cross-finned heat transfer surfaces. In: Proceedings of the III Minsk International Forum for Heat Transfer, vol. 2, pp. 150–154 (in Russian).

Romero-Mendez, R., Mihir SenYang, K.T., McClain, R., 2000. Effect of fin spacing on convection in a plate fin and tube heat exchanger. Int. J. Heat Mass Transfer.

Schlichting, H., Gersten, K., 2000. Boundary Layer Theory -8., rev. and enl. ed. Springer, Berlin, pp. 19–24.

White, F.M., 1988. Fluid Mechanics. McGraw-Hill, New York.

Zukauskas, A.A., 1982. Convection Heat Transfer in Heat Exchanger. Nauka, Moscow (in Russian).